Numerical Studies into Factors Affecting Structural Behaviour of Composite Cold-Formed Steel and Timber Flooring Systems

Dheeraj Karki*, Harry Far, Ali Saleh

School of Civil and Environmental Engineering, Faculty of Engineering and Information Technology, University of Technology Sydney (UTS), Sydney, Australia

Abstract:

Lightweight flooring system made up of cold-formed steel joist, and timber floorboard is widespread but the benefits of composite action that arise due to the interaction of top flange of cold-formed steel joist and the bottom surface of timber floorboard as a result of mobilising the shear connection are not considered in their design. A three-dimensional (3D) finite element model was developed and validated against the experimental results for cold-formed steel and particle board flooring system. The validated numerical model was used for parametric studies to investigate the influence of various factors that affect the structural behaviour of the composite flooring system. The results from the parametric studies showed that higher strength and stiffness values of engineered timber product, as well as their increased thickness, enhances the moment capacity and stiffness of the flooring system. The reduction in the spacing of the cold-formed steel joist was found to increase the stiffness and hence the load-carrying capacity of the flooring system. The high strength to weight ratio of cold-formed steel flooring system is also demonstrated in this study. A simplified design method is also proposed herein to predict flexural capacity of composite beams taking into account for the composite action. The finding in this study indicates that the design and construction of composite cold-formed steel and timber flooring system should be subjected to availability of the engineered timber product in the region, and the choice of timber floorboard thickness and joist spacing can be based on the ultimate strength and serviceability requirements of the flooring systems to make it cost-effective.

Keywords: *Cold-Formed Steel Joists; Timber based floorboards; Composite Floors; Finite Element Analysis; Composite action; Flexural Behaviour*

*Corresponding author: PhD candidate in School of Civil and Environmental Engineering, Faculty of Engineering and Information Technology, University of Technology Sydney (UTS), Building 11, Level 11, Broadway, Ultimo, NSW 2007 (PO Box 123), Email: Dheeraj.karki@student.uts.edu.au

1 INTRODUCTION

The use of cold-formed steel as load-bearing and non-load bearing members in a variety of lightweight construction for residential, commercial and industrial buildings has significantly increased over the past decades [1, 2]. The benefits of using cold-formed steel sections are high strength-to-weight ratio, ease of fabrication, and rapid installation [3, 4]. Recent studies [5, 6] have also highlighted the benefits of using cold-formed steel members in the building industry. The use of cold-formed steel joists with timber-based floorboards for the construction of lightweight flooring system in residential buildings is widespread. However, no design guidelines have been published yet for the flooring system to consider the beneficial effect of mobilising composite action on the flexural capacity [7, 8].

The demand for lightweight flooring systems in the building construction industry is increasing over the recent years [9]. Initially, the application of cold-formed steel joist was limited to domestic floors, but the increasing urbanisation is causing a shift from domestic buildings to mid-rise apartments, making it as the best alternative to conventional timber floor joists [10]. Lightweight flooring systems which are made up of cold-formed steel joist and timber-based floor panels can be an economical and durable solution for the construction of flooring systems for the construction industry due to ease of mass production and rapid installation [11]. Composite cold-formed steel and timber flooring systems can be assembled off-site and be fixed on-site in a modular way which will reduce the construction time [12]. Such flooring system also offers an advantage of high strength to weight ratio, which eventually reduces the self-weight of floors and less imposed load on the foundation [13]. Most recently Karki and Far [14] has discussed about the trends and developments in composite cold-formed steel floors. Fig.1 below shows a typical raised floor construction in a domestic building in Australia using cold-formed steel joists.

Fig. 1. A typical domestic raised floor system using cold-formed steel joists [15].

Several studies (e.g. Xu et al. [16], Xu and Tangorra [17], Parnell et al. [18]) evaluated the vibration performance of cold-formed steel lightweight floors. They investigated the key parameters that contribute to minimising floor vibrations without taking into account interaction between the timber floor-boards and cold-formed steel joist. Recently, researchers have started to explore the structural behaviour of this type of lightweight flooring system [8, 19]. Li et al. [20] demonstrated the structural performance of cold-formed steel and bamboo composite floors to replace concrete or wooden slabs in residential buildings. The experimental and numerical investigation on composite flooring systems comprising cold-formed steel joist with cross-laminated timber [12], particleboard [11, 19], and oriented strand board [8] demonstrated the potential for increased load carrying capacity and stiffness of composite flooring system when the shear connection is adequately provided taking into account the advantage of composite action. Far [21] also highlighted the importance of shear connection on composite flooring system comprising cold-formed steel and timber floorboards.

Experimental investigations alone can be time-consuming and costly to study all the associated factors that influence the strength and stiffness of the composite cold-formed steel flooring system [11, 22]. Hence the need for finite element analysis that can cover the behaviour of the flooring system as captured in the laboratory is essential to study broadly about the topic and for further development. As a result, this study presents numerical studies to investigate the influence of type and thickness of timber floorboards, as well as spacing of joist that affect the structural behaviour of the composite flooring system considering the benefits of composite action that arises between the interface of cold-formed steel joist and timber floor-boards. The four-point bending tests carried out by Kyvelou et al. [19] have been used to validate the numerical models.

2 DEVELOPMENT OF FINITE ELEMENT MODELS

Several researchers [2, 23, 24] have demonstrated the importance of nonlinear finite element analysis to study the structural behaviour and performance of cold-formed steel. Few recent studies [8, 11, 25] have utilised nonlinear finite element analysis to simulate the behaviour of composite flooring system comprising cold-formed steel joists. The numerical results from those studies were found to be close enough to experimental measurements. ANSYS 19.1 [26] was used for the numerical investigation in this study, incorporating all the material and push-out tests data from the testing conducted by Kyvelou et al. [19]. The actual experimental tests were conducted with a pair of cold-formed steel joists, but in this study, a single joist and effective width of timber floor-board as shown in Fig. 2 was modelled with the necessary boundary conditions applied on the axis of symmetry. This significantly helps to reduce the computational time of the finite element model. The developed finite element models were used to validate the physical beam tests as detailed in Kyvelou et al. [19], and hence the validated model was used for the parametric studies to investigate the influence of different parameters as outlined in Section 4 of this paper.

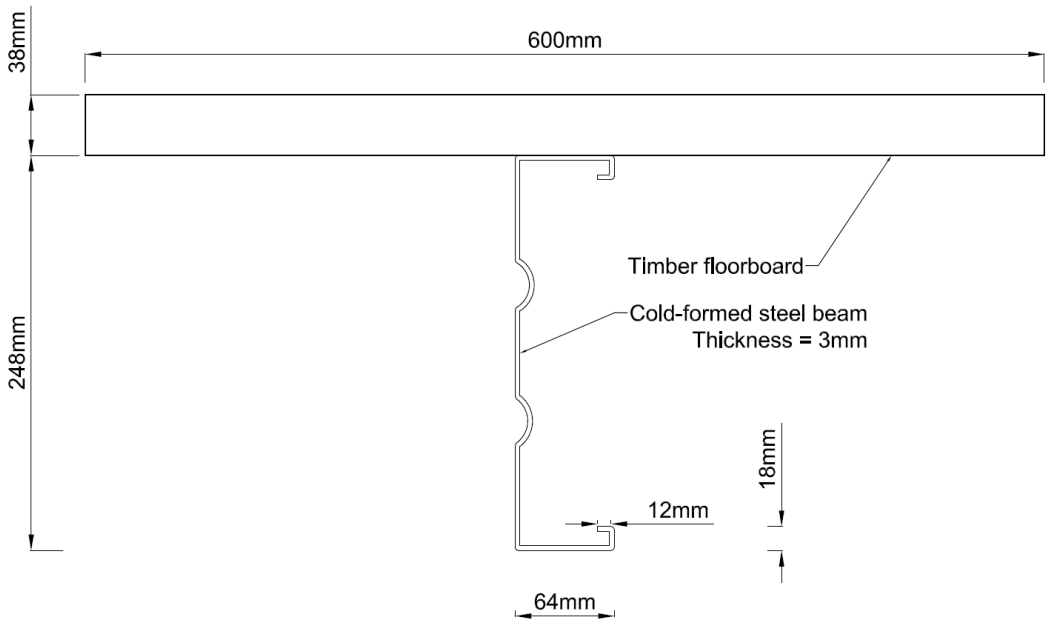

Fig. 2. Typical cross-section of composite CFST used in the numerical model.

2.1 Material Inputs

The material properties of the cold-formed steel joist and particle board adopted in this study were taken from the results of the material tests carried out by Kyvelou et al. [19]. The cold-formed steel material exhibits a multi-linear stress-strain curve in uniaxial tension as obtained from the tensile coupon tests. Since cold-formed steel typically does not indicate a clear yield point on its stress-strain curve, the two-stage Ramberg-Osgood model as proposed by Gardner and Ashraf [27] is chosen to model cold-formed steel. The summary of the mechanical properties of cold-formed steel is provided in Table 1. For cold-formed steel, Von Mises yield criterion is used with associative flow rule and isotropic hardening rule [28].

Table 1. Average measured mechanical properties of cold-formed steel

Material Characteristics	Value
Elastic modulus, E (MPa)	200000
Poisson's ratio, υ	0.3

Flat yield strength, $\sigma_{0.2}$ (MPa)	484
Corner Yield strength, $\sigma_{0.2}$ (MPa)	574
Tensile strength, σ_u (MPa)	559

Source: Adapted from Kyvelou et al. [19]

It should be noted that for the purpose of validation, elastic properties of particle board extracted by Kyvelou et al. [19] were adopted to simulate the response of cold-formed steel and particle board flooring system. The numerical results were compared with the results of experimental measurements [19], and the numerical studies carried out by Kyvelou et al. [11]. Once validation was successful, such comparative studies enabled the authors to conduct parametric studies to explore the benefits of using various engineered timber products available in the market. In the numerical analyses carried out by several researchers [8, 11, 12], isotropic behaviour of timber sheathing was considered, and a close agreement with the experimental results was reported. Hence, for the input of the FE model in this study, the average stiffness and strength properties of engineered timber products in the bending direction are utilised. Material properties of the particle board (PB) and other engineered timber products considered in the parametric studies are given in Tables 2 and 3.

Table 2. Average stiffness properties of engineered timber products used in this study

	Modulus of Elasticity (MPa)			**Poisson's ratio**
Engineered Timber Products	Bending	Compression	Tension	
Particleboard **[19]**	4100	2300	2100	0.2
Plywood **[29]**	6110	6124	6372	0.3
OSB **[30]**	5250	-	-	0.3
Laminated Moso Bamboo **[31]**	10,350	-	-	0.35
LVL **[32]**	13,500	-	-	0.44

Table 3. Average strength properties of engineered timber products used in this study

	Strength properties (MPa)		
Engineered Timber Products	Bending	Compression	Tension
Particleboard **[19]**	12.9	12.9	5.8
Plywood **[29]**	29.6	25.5	20.3
OSB **[30]**	21.2	-	-
Laminated Moso Bamboo **[33]**	77	77	90
LVL **[33]**	68	57	49

2.2 Element types and Meshing

SHELL181 element was used to simulate the cold-formed steel joists. SHELL181 is a four-node element with six degrees of freedom at each node: translation and rotation about x, y, and z-axes. This element is suitable for analysing nonlinear problems such as large rotation, large deformation, and large strain so the ultimate strength can be captured [28]. Several researchers [34, 35] have utilised this type of element in previous studies for modelling cold-formed steel structures.

SOLID185 element was used for modelling the timber floor-boards. It is an eight-node element with three degrees of freedom at each node: translation in x, y and z axes. The existing gap between adjacent floorboards was modelled with CONTA178 element. The element is defined by two nodes with an initial gap and represents contact and sliding between the two nodes. COMBIN39 element was used to model the self-drilling screws that act as the shear connection between the cold-formed steel joists and timber floorboards. COMBIN39 element is a unidirectional nonlinear spring element with nonlinear generalised force-deflection capability. The load-slip response of screws which were experimentally calculated by Kyvelou et al. [19], was utilised in this numerical investigation for the spring behaviour of COMBIN39 element.

Mapped mesh method was used to finely mesh the geometry with regular shape to get a more accurate analysis. The mesh size in the longitudinal direction of the model was set to be 10mm for the shell elements and 20mm for solid elements. The mesh size adopted in this study was in good agreement with the four-point bending test results as reported in Kyvelou et al. [19], so no further refinements were considered in this study.

2.3 **Contact Modelling and Boundary Conditions**

The interaction between the top flange of the cold-formed steel joist and the bottom surface of timber floorboards, and between the adjacent floorboards was modelled using surface-to-surface pair based contact elements. CONTA174 element is used to simulate the contact and sliding between the surfaces. Coulomb isotropic friction coefficient of 0.2 and 0.3 was defined between contacting surfaces of steel and timber, and timber and timber respectively as utilised by Kyvelou et al. [11] in their finite element analysis.

The 6000mm floor was supported across 5800mm span in a simply supported condition. In the experimental setup, at the position of support and loading points where the beam was subjected to high concentrated forces, it was stiffened locally to prevent web failure. Hence, in this FEA, rigid plates were connected to cold-formed steel joist at the position of concentrated forces. An artificially high elastic modulus 2000000 MPa (i.e., $10xE_{steel}$) was considered for the rigid plate. A simplified sketch that illustrate the four-point bending arrangement of the composite beam used in this numerical study is shown in Fig. 3, and an overview of the model geometry and boundary conditions is illustrated in Fig. 4.

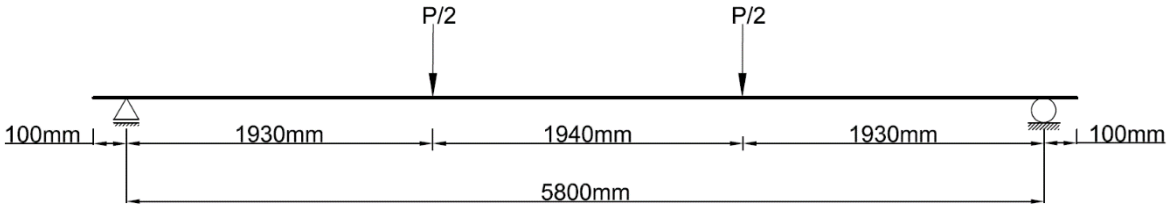

Fig. 3. Simplified sketch of four-point bendig test considered in this study.

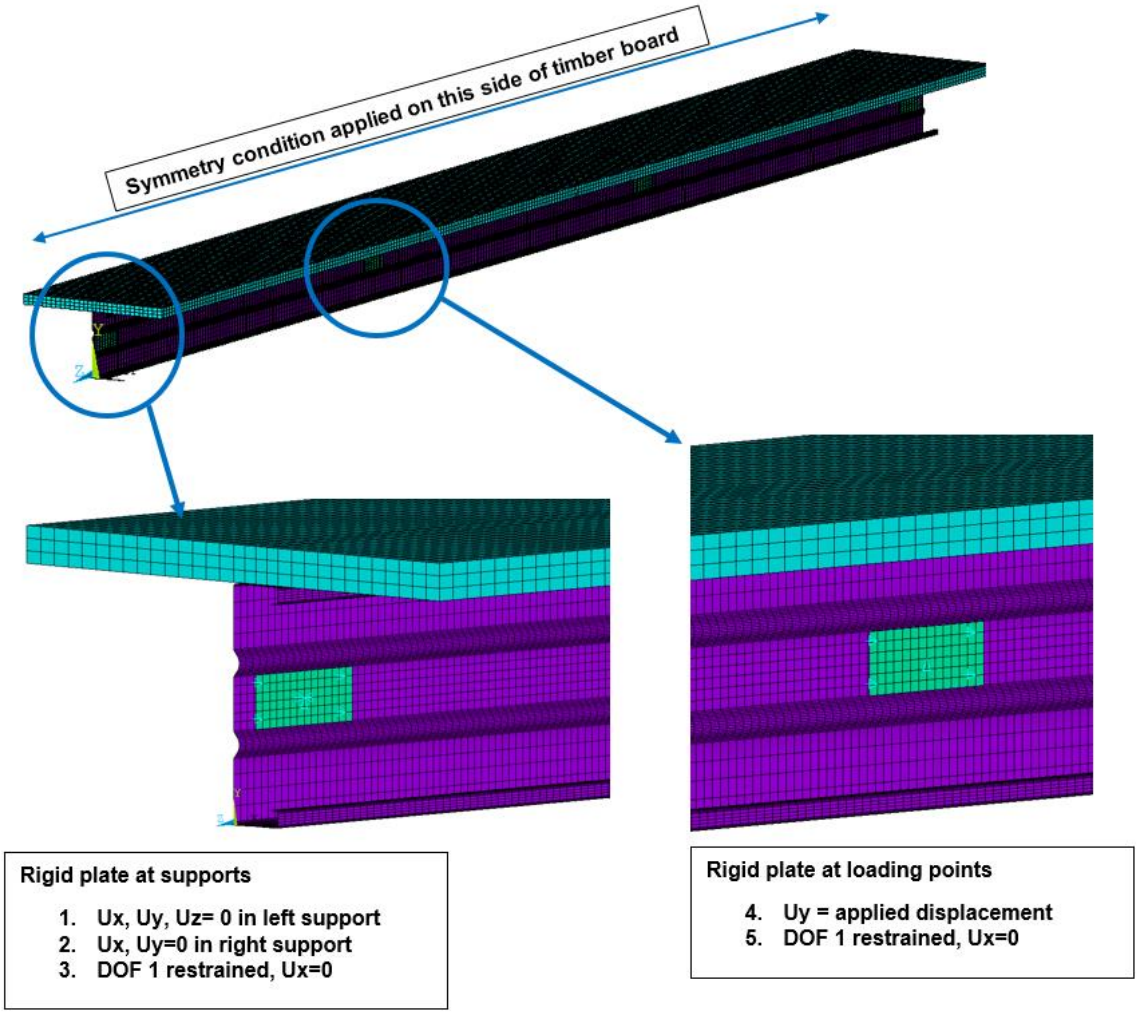

Fig. 4. Boundary conditions used in finite element analysis for numerical model validation.

2.4 **Initial Geometric Imperfections**

Many researchers [36-38] highlighted the importance of including geometric imperfections to capture the ultimate load capacity of structures accurately. The most common way used by researchers for the inclusion of geometric imperfections is to perform eigenvalue buckling analysis (EBA) firstly to obtain appropriate buckling mode shape, which is then included in the nonlinear analysis to define initial imperfection [39, 40]. But the study conducted by Haidarali and Nethercot [24] showed that utilising EBA for the determination of initial imperfections can be challenging for some sections when the interaction between local-distortional buckling arises. So a finite strip software CUFSM 3.12 [41] and sinusoidal functions were used in their study to generate the initial geometric imperfections. CUFSM is a cross-section and member elastic buckling analysis tool that can efficiently provide buckling modes and loads for any applied end action [41]. A similar approach was followed by Kyvelou et al. [11] on her study, and a good agreement of the experimental and numerical results in terms of ultimate strength and buckling behaviour of cold-formed steel beam were found. However, the studies carried out by some researchers [39, 42, 43] employed EBA to obtain appropriate mode shapes and then include them in the non-linear analysis also reported an excellent agreement between the experimental and numerical results. Hence it can be understood that the geometric imperfection can be included using the conventional method of feeding the Eigenmodes from EBA into non-linear analysis or the approach adopted by Haidarali and Nethercot [24].

In this study, EBA was carried out to predict appropriate Eigenmodes for local and distortional buckling. The local and distortional buckling modes were factored by measured magnitude in the tests. These buckling modes were then incorporated into the nonlinear analysis to consider the distribution of initial geometric imperfections. The magnitude of local and distortional imperfection was taken 0.1t and 0.3t (‘t’ is the thickness of cold-formed steel), respectively, as measured in the tests by Kyvelou et al. [19].

2.5 **Analysis assumptions**

For all the conducted analyses herein, large displacement static analysis was performed using the Newton-Raphson method taking into account material and geometrical nonlinearities. The models were loaded gradually in multiple steps based on displacement control procedure. Almost all the analyses had solution convergence issues because of nonlinearity in the system due to large deformation, material behaviour, and contact behaviour. Therefore, to overcome the convergence issues, nonlinear stabilisation (reduced stabilisation) technique was employed throughout the analyses. For the accuracy of the result, nonlinear stabilisation was activated in a multi-frame restart.

3 **VALIDATION OF FINITE ELEMENT MODELS**

The accuracy of the numerical model developed in this study was confirmed after the numerical results were validated against the experimental test results performed by Kyvelou et al. [19]. The validated model was then used for parametric studies to study the influence of the different type of engineered timber products, the thickness of floorboard and joist spacing. The cross-sectional shape, height (250mm), and thickness (3mm) of the cold-formed steel joist were kept constant.

Kyvelou et al. [19] conducted seven composite beam tests comprising cold-formed steel joists and particle board (PB) with alternative means of shear connection. Out of the seven tested flooring systems, two of them were used to validate the accuracy of the FE model developed in this study. Specimens B30-2 and B30-4 have been selected, and Table 4 shows the summary of those specimens with different means of shear connection.

Table 4. Summary of the tested system adopted for numerical model validation in this study

Specimen	CFS joist thickness (mm)	Screw spacing (mm)	Wood adhesive at floorboard joints	Structural adhesive at beam-board interface

B30-2	3	600	No	No
B30-4	3	300	No	No

Source: Adapted from Kyvelou et al. [19]

The comparison of typical observed failure mode of the specimen B30-2 is shown in Fig. 5. The tested specimen showed the distortional buckling of the top flange of CFS in the constant moment region between the screw connections and similar failure behaviour of CFS in the mid-span was captured in this study as shown in Fig. 5(c).

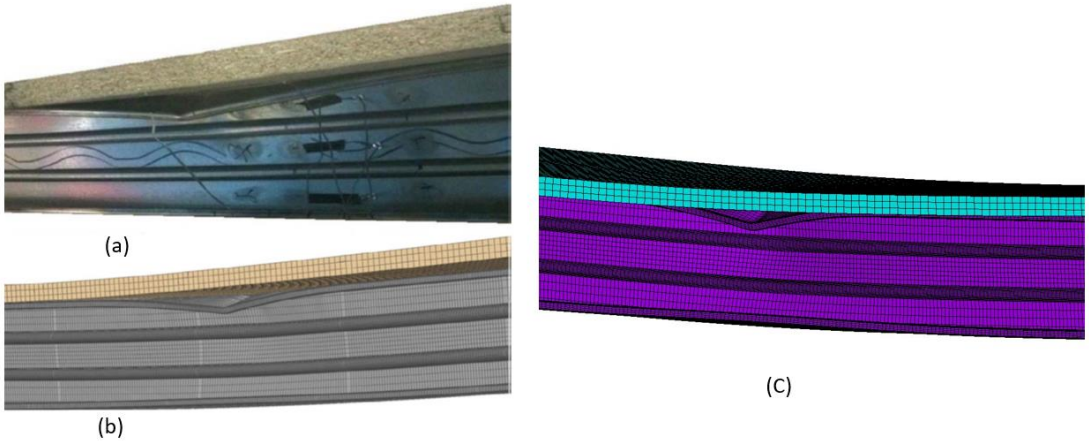

Fig. 5. Comparison of typical observed failure mode from; (a) Kyvelou et al. [19] Test, (b) Kyvelou et al. [11] FEA study, and (c) This study

Furthermore, the comparison of load-deflection responses and cross-section strain distribution at mid-span of the composite beam is shown in Fig. 6 and Fig. 7, respectively.

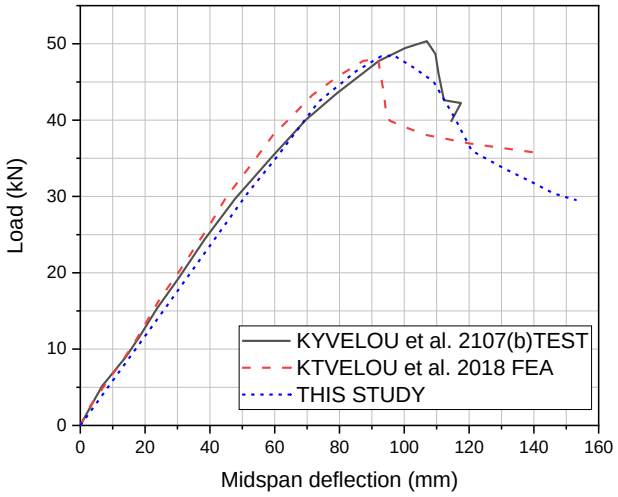

Fig. 6. Comparison of Load-deflection responses for Specimen B30-2.

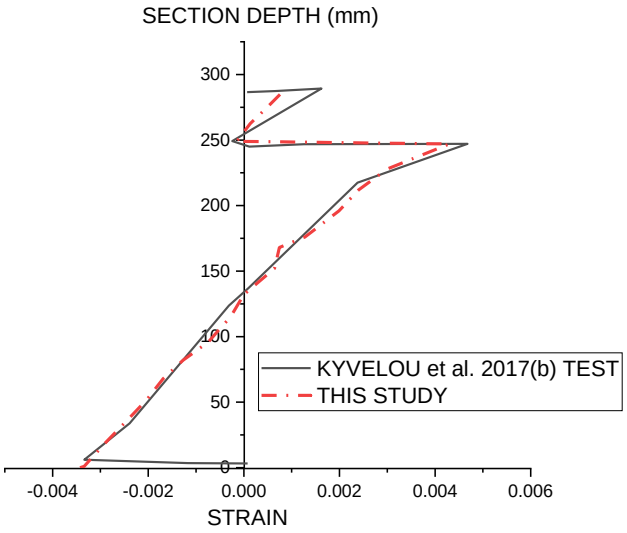

Fig. 7. Comparison of cross-sectional strain distributions at ultimate load for test and FEA at mid-span (For Specimen B30-2).

The ultimate load of the tested specimen was recorded to be 50kN with corresponding deflection 106.3mm [19]. In contrast, in this study, the ultimate load was obtained as 48kN with corresponding deflection 90mm similar to the one

reported by Kyvelou et al. [11]. The cross-sectional strain values obtained in this study is found to be linear from top to bottom and passing through zero at the neutral axis (NA). The captured values in this FEA were close to the values measured in the test and coincide through the neutral axis of the tested composite beam. Hence, from Figs. 4,5, and 6 it becomes apparent that the finite element model developed for this study is capable of predicting the structural behaviour as studied by Kyvelou et al. [19] and Kyvelou et al. [11].

In addition to the validation of B30-2, the comparison of the load-deflection response of specimen B30-4 is shown in Fig. 8 which further demonstrates that the developed numerical model is capable of predicting the load-carrying capacity of the tested composite beam specimen with acceptable accuracy.

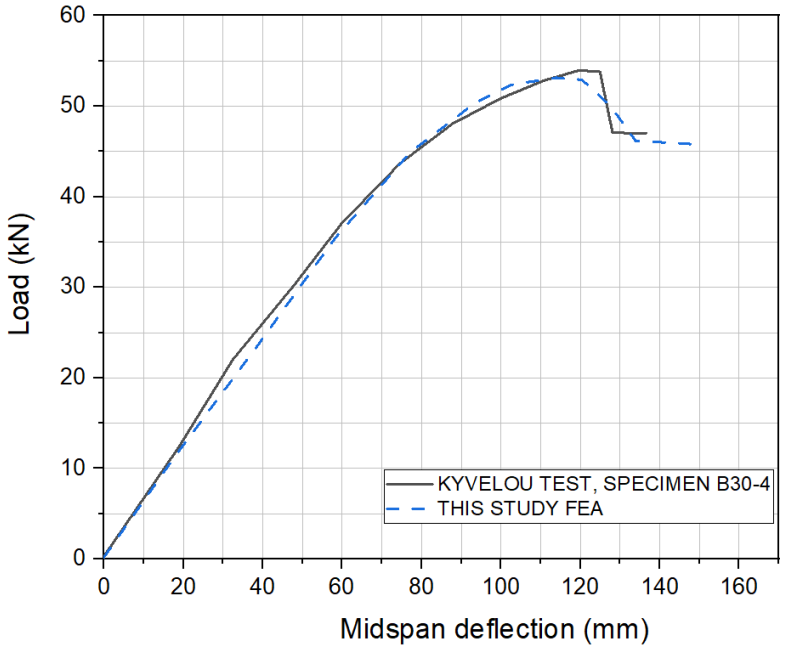

Fig. 8. Comparison of Load-deflection responses of Specimen B30-4.

Table 5 shows the comparisons between the four-point bending test carried out by Kyvelou et al. [19] and finite element analysis conducted in this study in terms of the ultimate moment capacity of the composite cold-formed steel and particle board

flooring system. The finite element models were found to predict the ultimate moment of both the specimens with 97% and 98% accuracy, respectively.

Table 1. Comparison of ultimate moment capacity between the four-point bending test and FEA

Specimen	**Kyvelou's Test** $M_{u,exp}$ **(kN.m)**	**This FEA Study** $M_{u,fea}$ **(kN.m)**	$M_{u,fea}/M_{u,exp}$
B30-2	48.56	47.2	0.97
B30-4	52.35	51.35	0.98

Thus, the finite element model results were found to be in a very good agreement with the four-point bending test measurements conducted by Kyvelou et al. [19]. Both studied specimens failed in-plane exhibiting distortional buckling of the top flange of cold-formed steel joist between fixings, as shown in Fig. 9.

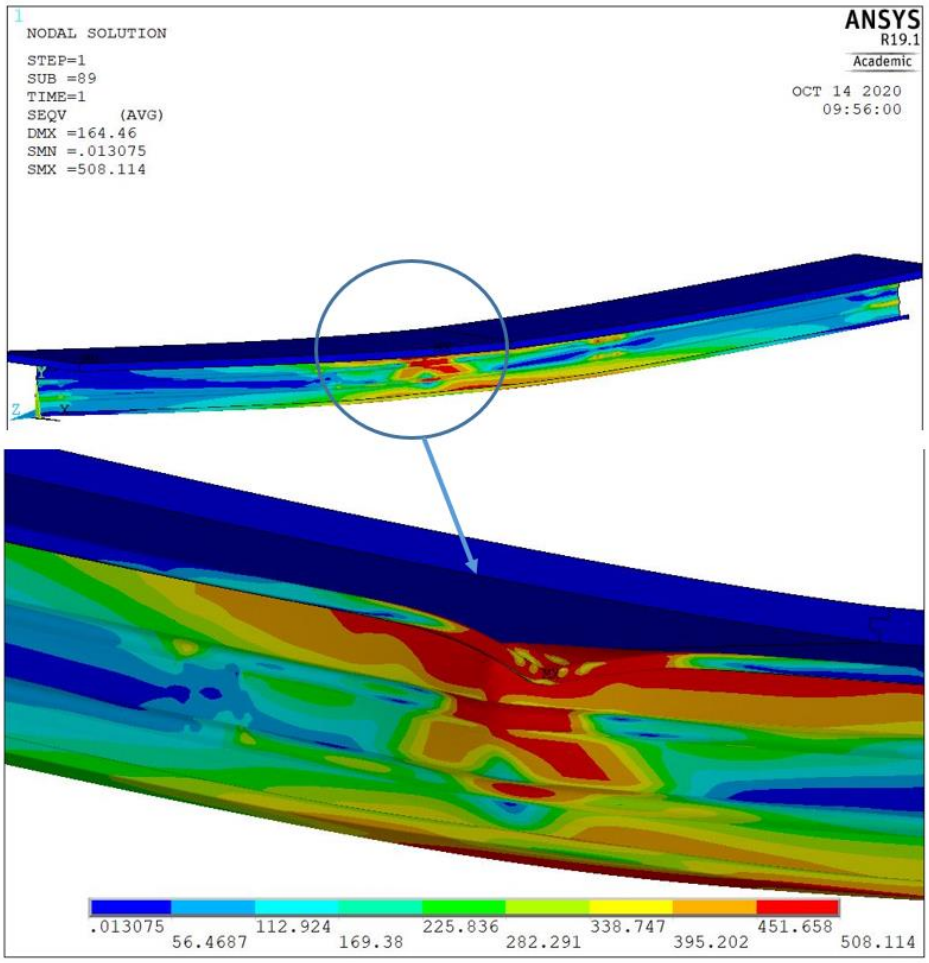

Fig. 9. Typical bending failure with distortional buckling between shear connectors at mid-span.

4 PARAMETRIC STUDIES AND RESULT DISCUSSIONS

The main objective of this study is to carry out parametric studies once the numerical model is validated. This section describes the influence of using different type of engineered timber products, varying the thickness of floorboard, and changing the spacing of the cold-formed steel joists on the flexural capacity of the studied composite cold-formed steel and timber flooring system. The ultimate moment capacity of the bare steel beam (without particleboard) was reported as 46.39 kN.m from the four-point bending test [19], and 43.6 kN.m from the numerical analysis [11]. In this study, the predicted ultimate moment capacity of the bare cold-formed steel joist was determined to be 42.1 kN.m. It has become apparent from the results

tabulated in Table 5 that composite action between the beam-board interfaces plays a significant role in enhancing the strength and stiffness of the composite beam. The parametric study results are compared in terms of the load-carrying capacity of the composite flooring system utilising the composite action at the shear connector's spacing of 600mm. The reason behind using a 600mm shear connection spacing is that it would simulate the partial shear connection between the CFS joist and the timber floorboard, which is the real scenario in terms of the practical case because the longitudinal slip between the components of the composite beam cannot be completely eliminated.

4.1 **Influence of engineered timber product**

The validated numerical model was used to investigate the potential utilisation of different engineered timber products available in the construction industry. The engineered timber products considered in this study were; structural plywood, oriented strand board (OSB), laminated Moso bamboo, and laminated veneer lumber (LVL). As expected, the elastic modulus and strength properties of engineered timber products influence the ultimate strength of the composite flooring system. The predicted ultimate moment capacities of the flooring system are tabulated in Table 6.

Table 2. Predicted ultimate moment capacities of CFST flooring system using various engineered timber products

Engineered timber products	Predicted moment capacity (kN.m)
Particleboard	47.2
OSB	47.9
Structural plywood	48.4
Laminated bamboo	48.9
LVL	49.4

Considering the results summarised in Table 6, it is understood that LVL, having the highest elastic modulus among all, yields the highest moment capacity while particle

board with lowest elastic modulus exhibits the lowest moment capacity for the studied flooring system. Hence, comparing the ultimate moment capacities of composite flooring system with shear connector spacing at 600mm showed that by replacing particleboard with LVL, laminated bamboo, structural plywood, and OSB the ultimate moment capacity of the flooring system could be improved by 4.5%, 3.5%, 2.6% and 2%, respectively. The load-deflection behaviour of the cold-formed steel composite beam with several timber floorboards is illustrated in Fig. 10. It is well known that the load-deflection curve exhibits the entire behaviour of the structural member from initial loads to the final loads or intial deformation to final deformation. The shape of the load-deflection curve depends on many factors including cross-section geometry, material properties, slenderness and load application [44]. In this study, the load-deflection response of particleboard after peak ultimate strength is different from other timber floorboards which can be attributed to the fact that the strength and stiffness properties of particleboard is relatively lesser than that of other timber floorboards. As can be depicted from Table 6 and Fig. 10, no substantial gain in the load-carrying capacity was observed in comparison with the benchmark study, i.e. cold-formed steel and particle board flooring system.

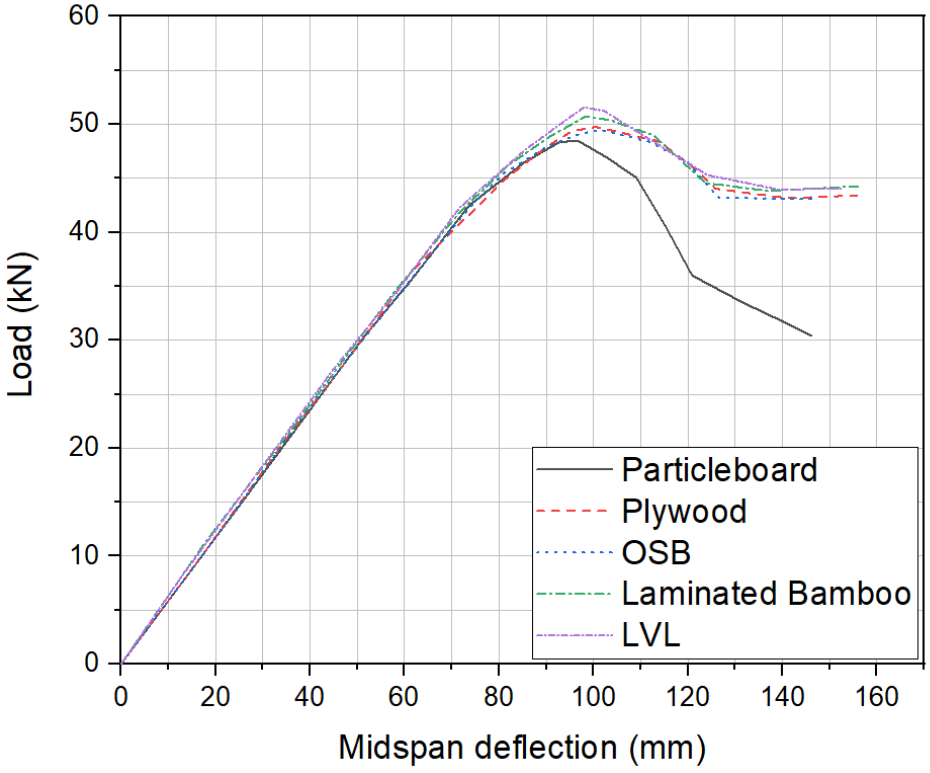

Fig. 10. Load and mid-span deflection curve of the composite CFS beam with different timber floorboard.

This finding indicates that changing timber floorboard would not be considered a feasible method in the construction of such flooring systems to achieve only 4 to 5 percent improvements in the current capability. The design of composite cold-formed steel and timber flooring systems may therefore be optimised by the use of locally available timber floorboards in the region.

4.2 **Influence of timber floorboard thickness**

Particle board (PB) has been chosen to investigate the influence of floorboard thickness on the structural behaviour of the composite flooring system with the shear connection spacing at 600mm. The validated numerical model used 38mm thick floorboard with the mechanical properties as tabulated in Tables 2 and 3. In the parametric study, the thickness of the particle board was changed to 20mm, 30mm, and 60mm with similar mechanical properties. It can be seen from Table 7 that for

20mm and 30mm thick particleboard, the moment capacity is almost similar and not of significant difference to that of 38mm particle board. In contrast, the use of 60mm particle board could be a better option to achieve a better performance in terms of strength and stiffness of such flooring system. However, the increasing thickness of the floorboard can significantly impact the total cost of the project.

Table 7. Predicted moment capacity and stiffness (under service load) of cold-formed steel and particleboard flooring system with different particleboard thickness

Thickness of particleboard	Predicted moment capacity (kN.m)	Stiffness (kN/mm) under service load
20mm	46.2	0.5678
30mm	46.5	0.5763
38mm	47.2	0.5781
60mm	49.1	0.5898
Bare steel beam	42	0.489

The stiffness (under service load) of the composite beam, which is the slope of the load-deflection curve, indicates that the composite beam can be stiffer up to 16%, 18%, 19% and 21% by the use of 20mm, 30mm, 38mm, and 60mm thick particleboard, respectively, through the utilisation of composite action at 600mm shear connection spacing. The load-deflection response of bare steel beam (without PB) and the composite beam is illustrated in Fig. 11. Comparing with the predicted ultimate load capacity of the bare steel beam, which is 43.6 kN, it is evident that the load capacity of the composite system enhanced by 9%, 10.5%, 12%, and 16.5% using 20mm, 30mm, 38mm, and 60mm of particle board in the composite beam respectively.

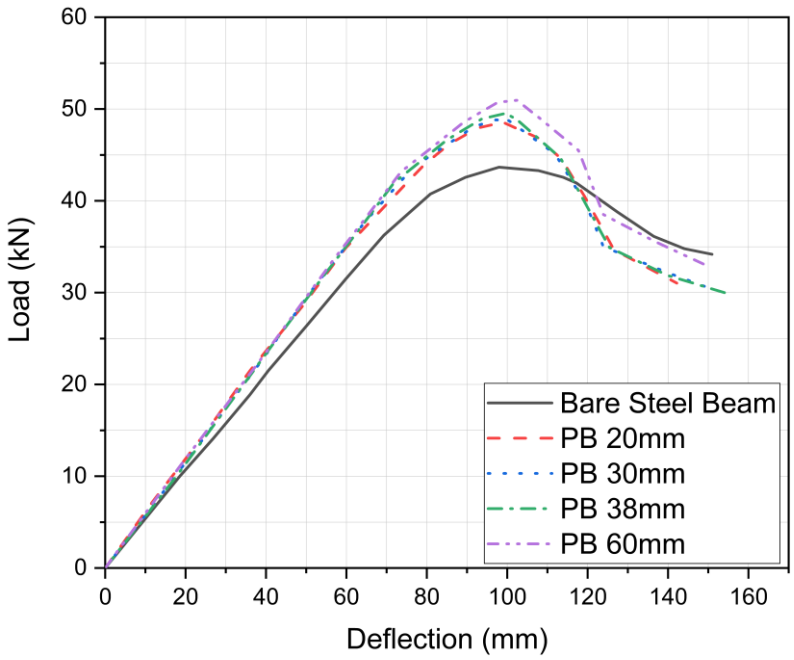

Fig. 11. Load and mid-span deflection curve of the composite CFS beam with different particleboard (PB) thickness and bare steel beam (Without PB)

All the conducted analyses for the varying thickness of particle board exhibited a similar failure mode of the CFS as depicted in Fig. 12. Distortional buckling between the shear connections was observed in the constant moment span of the composite beam.

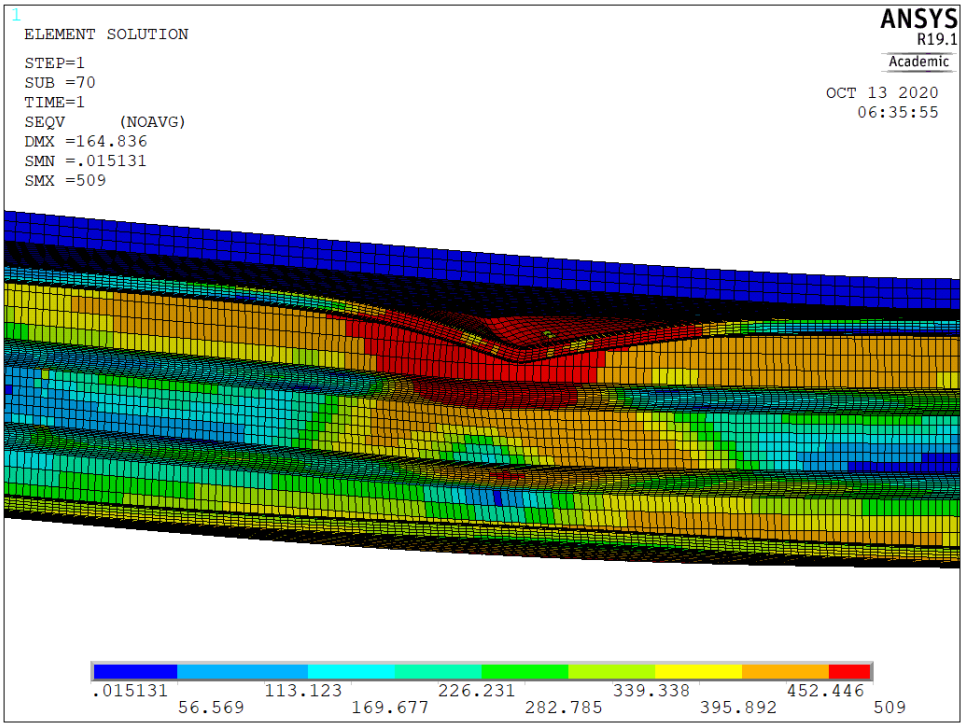

Fig. 12. Typical failure mode observed in CFS joist with different thickness of particleboard

4.3 **Influence of joist spacing**

The effect of joist spacing variation was investigated by analysing 6.0m long composite beam with two different effective particle board sheathing widths. The spacing of joist on the four-point bending test carried out by Kyvelou et al. [19] was 600mm. However, in this study, 400mm joist spacing was also chosen to find out the influence of joist spacing on the ultimate strength and serviceability of the composite beam. Fig. 13(b) shows the cross-section of the composite beam used for this study.

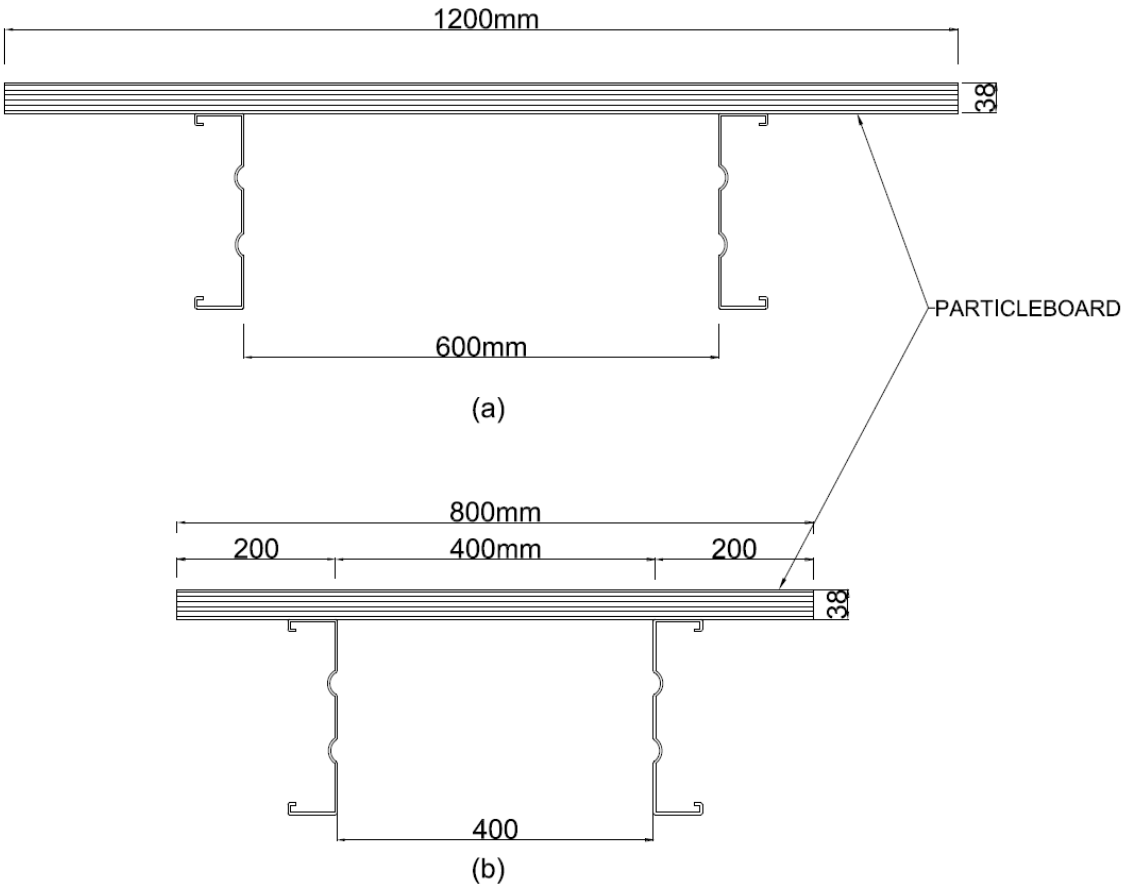

Fig. 13. Cross-section of cold-formed steel and particleboard composite beam (a) 600mm variation joist used in the 4-point bending test by Kyvelou et al. [19]; (b) 400mm spaced joist used in this study for numerical analysis.

It is apparent that 600mm wide composite beam has higher second moment of area and section modulus which will enhance the strength and stiffness of the beam. The predicted ultimate load, ultimate moment capacities, corresponding mid-span deflection, and stiffness of the composite beam with two different joist spacing are shown in Table 8. Comparing the composite beam results with bare steel beam in Table 7 it has become noticeable that the moment capacity of the composite system increased by 13% and 8%, respectively, for 600mm and 400mm wide beam. The numerical simulation of the symmetrical half of the composite beam model revealed that the estimated stiffness under service load and moment capacity of the 600mm

wide model were just 3.2% and 5% more than 400mm wide composite beam. The load and midspan deflection response of both the composite beam is shown in Fig. 14.

Table 8. Predicted moment capacity and stiffness of composite beams

Type of composite beam	Ultimate load (kN)	Predicted ultimate moment capacity (kN.m)	Mid-span deflection at ultimate load (mm)	Stiffness (kN/mm) under service load
600mm wide composite beam	48.9	47.24	96.7	0.5781
400mm wide composite beam	46.6	45	100.36	0.56

Results based on 38mm thick particle board

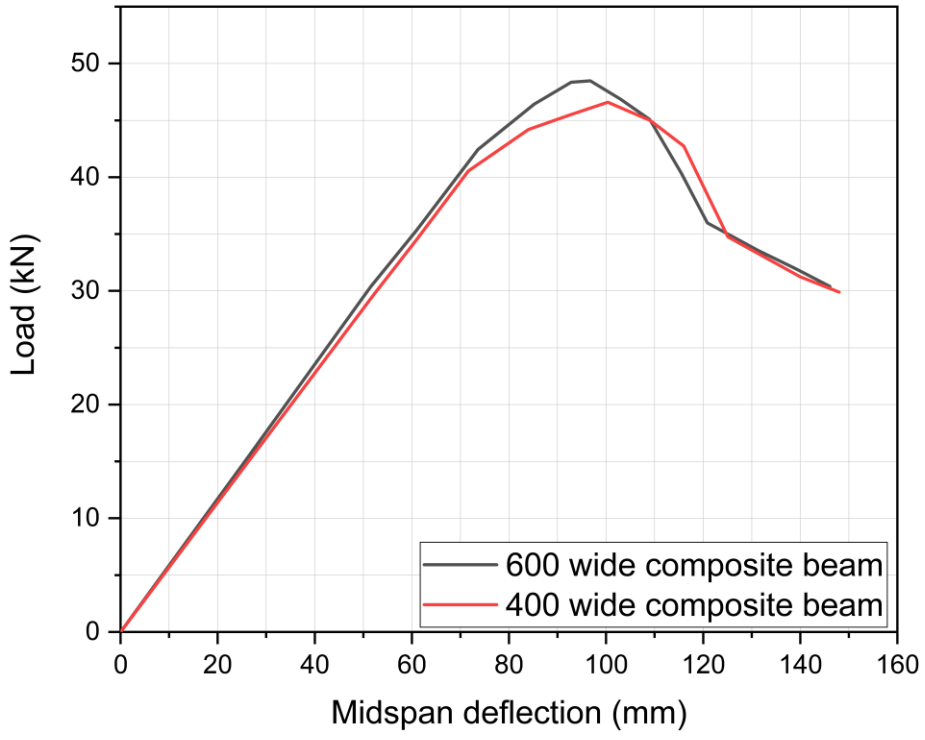

Fig. 14. Load and mid-span deflection response of 600mm and 400mm wide composite beams

Critical deformation at failure of top flange of the CFS in the constant moment span as depicted in Fig. 15 was observed for 400 wide composite beam similar to 600 wide beam (Fig. 5(c)).

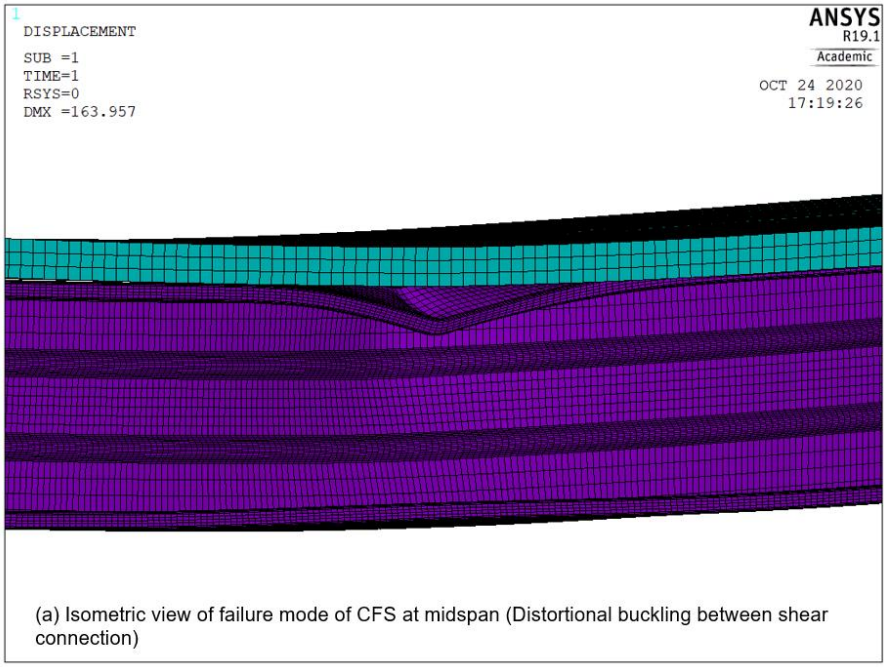

(a) Isometric view of failure mode of CFS at midspan (Distortional buckling between shear connection)

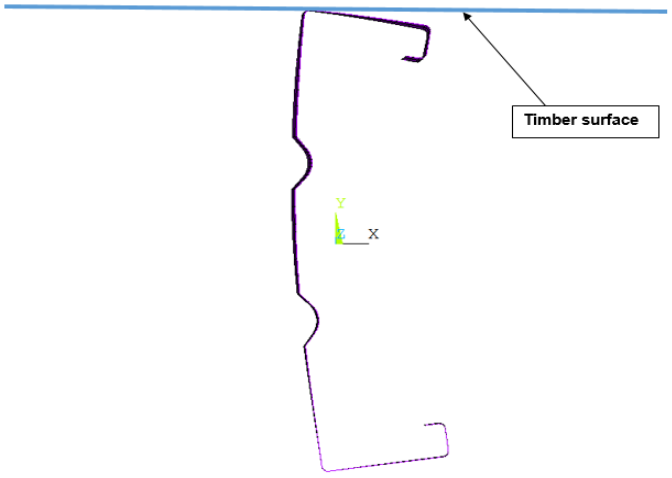

(b) Cross-section view at location of top flange buckling

Fig. 15. Observed failure mode of CFS at mid-span of 400mm wide composite beam (a) Isometric view ; (b) Cross-section view

To facilitate the comparision of the results for the two different joist spacings, a 1200mm width was adopted as reference width. This 1200mm width corresponds respectively to 2x600mm and 3x400mm joist spacings as shown in Table 9. The effective self-weight of the floor is also presented in Table 9. It can be observed that for 22% increase in self-weight of the floor, the load-carrying capacity increases by around 50% for 1.2 m wide floor with three joists (spacing at 400mm) than with two joists (spacing at 600mm). Hence this observation proves high strength to weight capacity of composite cold-formed steel and timber flooring system. However, it is worth noting that reducing the CFS joist spacing means increasing the cost of the floor construction. Therefore, in designing such flooring systems, the spacing of a joist is subjected to the required performance of the floor in terms of strength and serviceability.

Table 9. Load-carrying capacity normalised for 1200mmx6000mm composite beam

1200mm (width) x 6000mm (Length)		
No. of CFS joist	Self-weight of floor (kg/m^2)	Estimated load-carrying capacity (kN)
2	36.38	48.9
3	44.44	72.3

Self-weight and moment capacity based on 38 mm thick particle board

5 SIMPLIFIED CALULATION AND ANALYSIS

The model validation and parametric studies results indicate that the ultimate moment capacity and stiffness of the composite cold-formed steel and timber flooring system could be significantly improved by the utilisation of shear interaction between top flange of CFS joist and bottom surface of timber floorboard. A cold-formed steel joist that is sheathed with timber floorboard acts as composite T-beam. While

resisting bending in the composite member, timber floorboard acts as the compression flange and bottom of the cold-formed steel joist acts as tension flange. Because of non-rigid connection between the two members, full composite action may not exist and should not be assumed. Partial composite action takes place between the timber sheathing and CFS joist which contributes to the flexural capacity of floor joist. An analytical procedure of evaluation of composite behaviour of such floor system accounting for the parameters studied above is proposed here based on the validation and parametric studies.

As demonstrated in section 4, the composite action is likely influenced by the parameters like mechanical properties of timber floorboard, thickness of timber floorboard and joist spacing. It is well known that one of the major factor to influence the composite behaviour is the stiffness and spacing of screws. The ultimate flexural capacity of the composite T-beam can be obtained by equation (1)

$$M_u = \eta \times M_j \quad (1)$$

Where M_u is the ultimate flexural moment capacity of the composite beam, η is the coefficient of composite action (degree of partial shear connection) and M_j is the flexural moment of the CFS joist alone and can be calculated as $M_j = Z_e \times f_y$ in which Ze is the effective section modulus of CFS joist and fy is the yield strength of CFS.

So, $M_j = 85181(mm^3) \times 484(m.Pa) = 41227604N.mm = 41.22kN.m$

The effect of thickness of timber floorboard on coefficient of composite action is shown in Fig.16 and found to be increased approximately linearly with the increase of thickness.

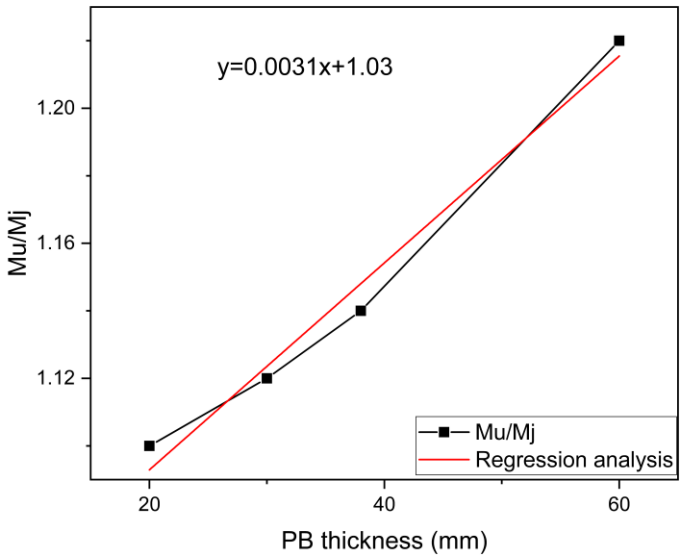

Fig. 16. Influence of thickness of floorboard on coefficient of composite action

From the regression analysis it is found that the coeffiecient of composite action, η can be expressed as

$$\eta = 0.0031 t_b + 1.03 \quad (2)$$

where t_b is the thickness of floorboard.

From section 4.3 it has become apparent that the effect of joist spacing (α) on coefficient of composite action can be generally expressed as

$$\eta_{JS600} = 1.05 \times \eta_{JS400} \quad (3)$$

The investigataion and model validation of specimen B30-2 and B30-4 as depicted in table 5 suggests the effect of screw spacing (β) on coefficient of composite action can be approximately expressed as

$$\eta_{ss\ 600} = 0.9 \times \eta_{ss\ 300} \quad (4)$$

Above investigation suggests that the coefficient of composite action, η can be expressed as

$$\eta = \alpha.\beta(0.0031 t_b + 1.03) \quad (5)$$

Equations (1) and (5) can be used to calculate ultimate flexural capacity of composite T beam. The comparison of the flexural capacity from FEA and proposed simplified method are presented in Table 10. M_u and M_{FEA} are the ultimate flexural capacity of composite cold-formed steel and timber T beam obtained from simplified method and FEA. It was found that the proposed simplified method agree well with the results from FEA.

Table 10. Comparison of ultimate flexural capacity by FEA and simplified method

T-beam	Thickness of floorboard (Tb)	α	β	η	M_u(kN.m)	M_{FEA} (kN.m)	M_u / M_{FEA}
600 wide beam; Screw spacing 600mm	38	1	1	1.14	46.99	47.24	0.99
600 wide beam; Screw spacing 300mm	38	1	1.11	1.26	51.93	51.35	1.01
600 wide beam; Screw spacing 600mm	60	1	1	1.21	49.87	49.1	1.01
600 wide beam; Screw spacing 600mm	20	1	1	1.092	45.01	46.2	0.97
400 wide beam; Screw spacing 600mm	38	0.95	1	1.08	44.5	45	0.98
				Average			0.992
				Standard deviation			0.0178
				Coefficient of variation			0.017

6 CONCLUSIONS

In this study, a finite element model has been developed and validated using four-point bending test results carried out by Kyvelou et al. [19]. The parametric numerical investigation was carried out to study the influence of utilisation of different types of engineered timber floorboards, variation in the floorboard thickness, and change in the joist spacing on the flexural behaviour of the flooring system. The investigation on the influence of different engineered timber floorboards indicates that variations in Young's moduli of different floorboard with same thickness yield to the variance in the ultimate moment capacity of the composite flooring system. In this study, up to 5% gain in the strength capacity of the flooring system was predicted by using LVL as a floorboard when compared with the benchmark study, i.e., flooring system with particleboard. Other timber floorboards considered in this study yielded less than 5% gain. Hence this suggests that modifying the timber floorboards alone would not seem to be a viable option to achieve just a 5% increase in the existing capacity in the design of such flooring systems.

The analysis on the effect of timber floorboard thickness shows that increase in the thickness of floorboard sheathing leads to enhanced moment capacity and stiffness of the flooring system. Thicker particleboard (60mm) was found to exhibit better structural performance than thinner particleboards. For instance, 60mm thick particle board was found to demonstrate 7% more moment capacity and 9% more stiffness in comparison to 20mm thick particleboard. However, the enhanced structural performance due to using thicker floorboard will negatively impact the cost of the project. Hence, the design of composite flooring system should be optimised depending on the availability of engineered timber around the region, where the flooring system would be constructed. In addition, the choice of suitable thickness would be governed by the loading requirements for the flooring system.

On reducing the joist spacing from 600mm to 400mm and increasing the number of CFS floor joists in a given size of a floor, the ultimate moment capacity of the flooring system was enhanced by around 50%. This finding reveals that the load-carrying capacity of the flooring system can be significantly improved by optimising the spacing of the CFS joists when designing such floors.

From the outcomes of this numerical study and proposed simplified method, it has become apparent that the distinction between the bare steel beam and the composite beam indicates that there is ample proof to consider the composite behaviour in the composite cold-formed steel and timber flooring system and the benefits to be gained in terms of strength and stiffness.

References

[1] Young, B. and Rasmussen, K. J. R., "Tests of Fixed-Ended Plain Channel Columns," *Journal of structural engineering,* vol. 124, no. 2, pp. 131-139, 1998.doi:10.1061/(ASCE)0733-9445(1998)124:2(131)

[2] Kankanamge, N. D. and Mahendran, M., "Behaviour and design of cold-formed steel beams subject to lateral–torsional buckling," *Thin-Walled Structures,* vol. 51, pp. 25-38, 2012/02/01/ 2012.https://doi.org/10.1016/j.tws.2011.10.012

[3] Hancock, G. J., *Design of Cold-formed Steel Structures: To Australian/New Zealand Standard AS/NZS 4600: 1996*. Australian Institute of Steel Construction, 1998.

[4] Wang, L. and Young, B., "Design of cold-formed steel channels with stiffened webs subjected to bending," *Thin-Walled Structures,* vol. 85, pp. 81-92, 2014/12/01/ 2014.https://doi.org/10.1016/j.tws.2014.08.002

[5] Far, H., Saleh, A., and Firouzianhaji, A., "A simplified method to determine shear stiffness of thin walled cold formed steel storage rack frames," *Journal of Constructional Steel Research,* vol. 138, pp. 799-805, 2017/11/01/ 2017.https://doi.org/10.1016/j.jcsr.2017.09.012

[6] Saleh, A., Far, H., and Mok, L., "Effects of different support conditions on experimental bending strength of thin walled cold formed steel storage upright frames," *Journal of constructional steel research,* vol. 150, pp. 1-6, 2018.https://doi.org/10.1016/j.jcsr.2018.07.031

[7] Kyvelou, P., Gardner, L., and Nethercot, D. A., "Design of Composite Cold-Formed Steel Flooring Systems," *Structures,* vol. 12, pp. 242-252, 2017.10.1016/j.istruc.2017.09.006

[8] Zhou, X., Shi, Y., Xu, L., Yao, X., and Wang, W., "A simplified method to evaluate the flexural capacity of lightweight cold-formed steel floor system

with oriented strand board subfloor," *Thin-Walled Structures,* vol. 134, pp. 40-51, 2019.10.1016/j.tws.2018.09.006
[9] NASH, "General guide to steel- framed building," National Association of Steel-Framed Housing, Victoria2007.
[10] Australian steel institute. (2019, 10/07/2019). *Growth in light gauge steel*.
[11] Kyvelou, P., Gardner, L., and Nethercot, D. A., "Finite element modelling of composite cold-formed steel flooring systems," *Engineering Structures,* vol. 158, pp. 28-42, 2018.10.1016/j.engstruct.2017.12.024
[12] Loss, C. and Davison, B., "Innovative composite steel-timber floors with prefabricated modular components," *Engineering Structures,* vol. 132, pp. 695-713, 2017.10.1016/j.engstruct.2016.11.062
[13] Loss, C., Piazza, M., and Zandonini, R., "Connections for steel–timber hybrid prefabricated buildings. Part II: Innovative modular structures," *Construction and Building Materials,* vol. 122, pp. 796-808, 2016/09/30/ 2016.https://doi.org/10.1016/j.conbuildmat.2015.12.001
[14] Karki, D. and Far, H., "State of the art on composite cold-formed steel flooring systems," *Steel Construction*.https://doi.org/10.1002/stco.202000026
[15] Stratco Australia. (2019, 1 October). *Steel framing-Tuffloor framing*.
[16] Xu, L., Ling, Z., Xie, W., and Schuster, R., "Dynamic behaviour of floors with cold-formed steel joists," in *International Speciality Conference on Cold-Formed Steel Structures*, 2000, 2000.
[17] Xu, L. and Tangorra, F. M., "Experimental investigation of lightweight residential floors supported by cold-formed steel C-shape joists," *Journal of Constructional Steel Research,* vol. 63, no. 3, pp. 422-435, 2007.10.1016/j.jcsr.2006.05.010
[18] Parnell, R., Davies, B. W., and Xu, L., "Vibration Performance of Lightweight Cold-Formed Steel Floors," *Journal of structural engineering,* vol. 136, pp. 645-653, 2010.10.1061/(ASCE)ST.1943-541X.0000168
[19] Kyvelou, P., Gardner, L., and Nethercot, D. A., "Testing and Analysis of Composite Cold-Formed Steel and Wood−Based Flooring Systems," *Journal of Structural Engineering,* vol. 143, no. 11, 2017.10.1061/(asce)st.1943-541x.0001885
[20] Li, Y., Shen, H., Shan, W., and Han, T., "Flexural behavior of lightweight bamboo–steel composite slabs," *Thin-Walled Structures,* vol. 53, pp. 83-90, 2012.10.1016/j.tws.2012.01.001
[21] Far, H., "Flexural Behavior of Cold-Formed Steel-Timber Composite Flooring Systems," *Journal of structural engineering,* vol. 146, no. 5, p. 06020003, 2020.doi:10.1061/(ASCE)ST.1943-541X.0002600
[22] Queiroz, F. D., Vellasco, P. C. G. S., and Nethercot, D. A., "Finite element modelling of composite beams with full and partial shear connection," *Journal of Constructional Steel Research,* vol. 63, no. 4, pp. 505-521, 2007/04/01/ 2007.https://doi.org/10.1016/j.jcsr.2006.06.003
[23] Yu, C. and Schafer, B. W., "Simulation of cold-formed steel beams in local and distortional buckling with applications to the direct strength method,"

Journal of Constructional Steel Research, vol. 63, no. 5, pp. 581-590, 2007/05/01/ 2007.https://doi.org/10.1016/j.jcsr.2006.07.008

[24] Haidarali, M. R. and Nethercot, D. A., "Finite element modelling of cold-formed steel beams under local buckling or combined local/distortional buckling," *Thin-Walled Structures,* vol. 49, no. 12, pp. 1554-1562, 2011/12/01/ 2011.https://doi.org/10.1016/j.tws.2011.08.003

[25] Majdi, Y., Hsu, C.-T. T., and Zarei, M., "Finite element analysis of new composite floors having cold-formed steel and concrete slab," *Engineering Structures,* vol. 77, pp. 65-83, 2014/10/15/ 2014.https://doi.org/10.1016/j.engstruct.2014.07.030

[26] Ansyc Inc., "Academic Research Mechanical, Release 19.1," ed: Ansys Incorporation, Canonsburg, PA,2009, 2019.

[27] Gardner, L. and Ashraf, M., "Structural design for non-linear metallic materials," *Engineering Structures,* vol. 28, no. 6, pp. 926-934, 2006/05/01/ 2006.https://doi.org/10.1016/j.engstruct.2005.11.001

[28] Ansys Inc., "Theory Reference for the Mechanical APDL and Mechanical Applications," ed: Ansys Incorporation, Canonsburg, PA, 2009.

[29] Arriaga-Martitegui, F., Peraza-Sánchez, F., and García-Esteban, L., "Characteristic values of the mechanical properties of radiata pine plywood and the derivation of basic values of the layers for a calculation method," *Biosystems Engineering,* vol. 99, no. 2, pp. 256-266, 2008/02/01/ 2008.https://doi.org/10.1016/j.biosystemseng.2007.10.004

[30] Thomas, W. H., "Concentrated Load Capacity and Stiffness of Oriented Strand Board: Calculation versus Test," vol. 128, no. 7, pp. 908-912, 2002.doi:10.1061/(ASCE)0733-9445(2002)128:7(908)

[31] Bai, X., Lee, A. W., Thompson, L. L., and Rosowsky, D. V., "Finite element analysis of Moso bamboo-reinforced southern pine OSB composite beams," *Wood and fiber science,* vol. 31, no. 4, pp. 403-415, 1999.

[32] Janowiak, J. J., Hindman, D. P., and Manbeck, H. B., "Orthotropic behavior of lumber composite materials," *Journal of wood fibre science,* vol. 33, no. 4, pp. 580-594, 2001.

[33] Sharma, B., Gatóo, A., Bock, M., and Ramage, M., "Engineered bamboo for structural applications," *Construction and Building Materials,* vol. 81, pp. 66-73, 2015/04/15/ 2015.https://doi.org/10.1016/j.conbuildmat.2015.01.077

[34] Xu, L., Sultana, P., and Zhou, X., "Flexural strength of cold-formed steel built-up box sections," *Thin-Walled Structures,* vol. 47, no. 6, pp. 807-815, 2009/06/01/ 2009.https://doi.org/10.1016/j.tws.2009.01.005

[35] Ren, W.-X., Fang, S.-E., and Young, B., "Analysis and design of cold-formed steel channels subjected to combined bending and web crippling," *Thin-Walled Structures,* vol. 44, no. 3, pp. 314-320, 2006/03/01/ 2006.https://doi.org/10.1016/j.tws.2006.03.009

[36] Chou, S. M., Chai, G. B., and Ling, L., "Finite element technique for design of stub columns," *Thin-Walled Structures,* vol. 37, no. 2, pp. 97-112, 2000/06/01/ 2000.https://doi.org/10.1016/S0263-8231(00)00018-5

[37] Dubina, D. and Ungureanu, V., "Effect of imperfections on numerical simulation of instability behaviour of cold-formed steel members," *Thin-Walled Structures,* vol. 40, no. 3, pp. 239-262, 2002/03/01/ 2002.https://doi.org/10.1016/S0263-8231(01)00046-5

[38] Ellobody, E., Feng, R., and Young, B., *Finite Element Analysis and Design of Metal Structures*. Oxford, UNITED STATES: Elsevier Science & Technology, 2013.

[39] Wang, H. and Zhang, Y., "Experimental and numerical investigation on cold-formed steel C-section flexural members," *Journal of Constructional Steel Research,* vol. 65, no. 5, pp. 1225-1235, 2009/05/01/ 2009.https://doi.org/10.1016/j.jcsr.2008.08.007

[40] Seo, J. K., Anapayan, T., and Mahendran, M., "Initial Imperfection Characteristics of Mono-Symmetric LiteSteel Beams for Numerical Studies," in *Proceedings 5th International Conferance on Thin-Walled Structures:ICTWS 2008*, 2008, Brisbane.

[41] CUFSM Version 3.12 by Ben Schafer, ed. Department of Civil Engineering, Johns Hopkins University, 2006, p. /http://www.ce.jhu.edu/bschafer/cufsm/.

[42] Pham, C. H. and Hancock, G. J., "Numerical simulation of high strength cold-formed purlins in combined bending and shear," *Journal of Constructional Steel Research,* vol. 66, no. 10, pp. 1205-1217, 2010/10/01/ 2010.https://doi.org/10.1016/j.jcsr.2010.04.014

[43] Laím, L., Rodrigues, J. P. C., and Silva, L. S. d., "Experimental and numerical analysis on the structural behaviour of cold-formed steel beams," *Thin-Walled Structures,* vol. 72, pp. 1-13, 2013/11/01/ 2013.https://doi.org/10.1016/j.tws.2013.06.008

[44] Anwar, N. and Najam, F. A., "Chapter Six - Ductility of Cross-Sections," in *Structural Cross Sections*, Anwar, N. and Najam, F. A., Eds.: Butterworth-Heinemann, 2017, pp. 391-481.